Published in "Macromolecular Chemistry and Physics 218 (22): 1700302, 2017"
which should be cited to refer to this work.

Phase Segregation in Supramolecular Polymers Based on Telechelics Synthesized via Multicomponent Reactions

Ansgar Sehlinger, Nikolai Bartnick, Ilja Gunkel, Michael A. R. Meier, and Lucas Montero de Espinosa**

The properties of supramolecular polymers in the solid state are strongly dependent on the binding strength of the supramolecular motifs used; however, It has been previously shown that the nanostructure of supramolecular polymers plays an equally important role. Supramolecular polymers are commonly synthesized via end-group functionalization of low-glass transition telechelics with supramolecular units. In these systems, the binding motifs segregate from the soft telechelic backbone and form a hydrogen bonded crystalline hard phase that provides physical cross-links. To date, the reported synthetic approaches do not permit the introduction of a wide variety of supramolecular units with low synthetic effort, which would facilitate studying the structure-property relationships. The use of the Passerini and Ugi multicomponent reactions to synthesize various poly(ethylene-*co*-butylene) telechelics with diverse amide end-groups is reported. The thermal properties of the supramolecular polymers obtained through their solid-state assembly are investigated and their nanophase-segregation is studied, which is dictated by the end-group volume fraction and the amide–amide hydrogen bonding.

1. Introduction

Supramolecular polymers are a broad class of macromolecules in which the monomeric units are held together through non-covalent interactions.[1] These materials are typically based on H-bonding interactions, metal-ligand complexation, ion pairing, or pi–pi stacking, displaying a wide range of binding strengths that vary from very weak to covalent-like.[1] The possibility of addressing these reversible interactions with stimuli such as UV-light, sonication, or variations of temperature and pH makes supramolecular polymers a very attractive platform for the development of stimuli-responsive materials.[2–5] While using strongly binding supramolecular motifs such as the ureidopyrimidinone (UPy) dimer[6–8] or multidentate pyridine-based ligand-metal complexes[9] leads to very high apparent molecular weights and good material properties, the responsiveness of such materials is somewhat limited, as high temperatures are necessary to shift the equilibrium to the monomer side.[10,11] More weakly binding supramolecular motifs on the other hand display rapid switching on account of their high sensitivity to external stimuli, but do not provide mechanical integrity unless they are supported by phase segregation phenomena.[12,13] A common approach to overcome this intrinsic limitation thus relays on kinetically trapping the dynamic bonds into crystalline phases formed by the supramolecular motifs, which has been typically achieved by equipping low glass transition (T_g) telechelic macromonomers with, e.g., hydrogen bonding end-groups such as 4-urazoyl benzoic acid,[14–16] benzoic acid derivatives,[17,18] nucleobases,[19–21] urea and urethane groups,[22,23] or carboxylic acid-pyridine pairs.[24] The assembly of such monomers and subsequent crystallization-driven phase segregation of the supramolecular motifs produces elastomer-like materials with mechanical properties largely dominated by the crystalline hard phase.[24] Additionally, it has been shown that the crystallization of supramolecular motifs attached to the end-groups of telechelic macromonomers is strongly influenced by the molarity[15,25,26] and geometry[27,28] of the supramolecular units.

In order to develop highly responsive supramolecular polymers, it is therefore desirable to find binding motifs with low association constants and high crystallinity which, ideally, would be prepared through synthetically undemanding protocols. In this regard, the Passerini and Ugi multicomponent reactions (MCRs) match these two requirements as they lead to (hydrogen bonding) amide derivatives in one synthetic step with 100% atom economy in case of the Passerini reaction and water as only by-product in the case of the Ugi reaction.[29,30] MCRs have been used in the synthesis of very diverse macromolecular architectures[31–34] including linear,[35,36] branched and dendritic,[37,38] precisely sequence-defined,[39,40] polymers and have been shown to be useful for polymer end-group/side chain functionalization[41,42] on account of their high efficiency. Most importantly, MCRs offer rapid access to diverse structures

Dr. A. Sehlinger, N. Bartnick, Prof. M. A. R. Meier
Laboratory of Applied Chemistry
Institute of Organic Chemistry (IOC)
Karlsruhe Institute of Technology (KIT)
Materialwissenschaftliches Zentrum MZE
Straße am Forum 7, 76131 Karlsruhe, Germany
E-mail: michael.meier2@kit.edu
Dr. I. Gunkel, Dr. L. Montero de Espinosa
Adolphe Merkle Institute
University of Fribourg
Chemin des Verdiers 4, CH-1700 Fribourg, Switzerland
E-mail: lucas.montero@unifr.ch

by component choice, which is particularly useful for establishing structure/property relationships and, in the present work, to study the effect of various amide end-groups on the phase segregation behavior of low molecular weight telechelics. We thus report here the synthesis of a family of telechelics that share the same poly(ethylene-*co*-butylene) (PEB) backbone but display different amide derivatives as end-groups and study their phase segregation behavior. The hydrophobic, amorphous PEB backbone was chosen for its well-known propensity to phase segregate when covalently linked to polar and crystalline groups,[7,10,24] and both the Passerini and the Ugi MCRs were used to functionalize its end-groups with diverse amide derivatives. This synthetic approach was also chosen on the basis of the high crystallinity of most small molecules synthesized via Passerini and Ugi MRCs,[43,44] which were expected to provide a driving force for phase segregation.

2. Experimental Section

2.1. Materials

Hydroxyl-terminated poly(ethylene-*co*-butylene) (M_n = 3100 g mol^{-1}; polydispersity index = 1.05) was kindly donated by Cray Valley SA (Krasol HLBH-P 3000). The following chemicals were used as received: succinic anhydride (≥99%, Sigma-Aldrich), pyridine (≥99%, Sigma-Aldrich), 4-(dimethylamino) pyridine (≥99%, Sigma-Aldrich), acetaldehyde **1a** (≥99%, Sigma-Aldrich), isobutyraldehyde **1b** (≥99%, Sigma-Aldrich), phenylacetaldehyde **1c** (≥95%, Sigma-Aldrich), lauric aldehyde **1d** (≥95%, Sigma-Aldrich), *tert*-butyl isocyanide **2a** (98%, Sigma-Aldrich), benzyl isocyanide **2b** (98%, Sigma-Aldrich), 2-naphthyl isocyanide **2c** (95%, Sigma-Aldrich), *n*-propylamine **3a** (98%, Sigma-Aldrich), octadecylamine **3b** (≥99%, Sigma-Aldrich), phosphorous(V) oxychloride (99%, Sigma-Aldrich), ethyl formate (97%, Sigma-Aldrich), diisopropylamine (≥99.5%, Sigma-Aldrich), 1-bromodocosane (>98%, TCI), hexadecyltrimethylammonium bromide (≥98%, Sigma-Aldrich), sodium azide (reagent grade, Fisher Chemical), palladium on activated charcoal (10% Pd basis, Sigma-Aldrich). All solvents (HPLC quality) were used without further purification.

2.2. Characterization

^{1}H-NMR spectra were recorded on a Bruker AVANCE DPX spectrometer operating at 300 MHz. $CDCl_3$ was used as solvent and the resonance signal at 7.26 ppm (^{1}H) served as reference for the chemical shift δ. Differential scanning calorimetry (DSC) studies were carried out with a Mettler–Toledo STAR system under nitrogen atmosphere using a sample mass of ≈5 mg. The glass transition temperature T_g is reported as the midpoint of the step change in the heat capacity and the melting point is reported as the minimum of the endothermic peak. Small-angle X-ray (SAXS) spectra were recorded with a NanoMax-IQ camera (Rigaku Innovative Technologies, Auburn Hills, MI, USA). The samples were introduced in quartz capillaries (1 mm ∅) and kept in vacuum at −20 °C during the measurements using a Julabo F25-ME cooling/heating system. Raw data were processed according to standard procedures, and the scattering spectra (1d) are presented as a function of the momentum transfer $q = 4\pi \cdot \lambda\text{-}1 \cdot \sin(\theta/2)$, where θ is the scattering angle and λ = 0.1524 nm is the photon wavelength. Size exclusion chromatography (SEC) measurements were carried out on an Agilent Technologies 1200 system equipped with a Wyatt Optilab rEX differential refractive index (dRI) detector and a Wyatt miniDAWN TREOS multiangle laser light scattering (MALLS) detector. The column system was composed of an Agilent 5 µm MIXED-C guard column and a 5 µm MIXED-D (200–400 000 g mol^{-1}) column from Agilent. Tetrahydrofuran (THF) was employed as solvent/eluent and the measurements were carried out at 30 °C with a flow rate of 1 mL min^{-1}. The number average molecular weight and dispersity indexes were determined against poly(styrene) standards. Atomic force microscopy (AFM) was performed on a JPK Nanowizard II with a JPK Advanced SPM control station operated in tapping mode using rectangular Al-coated silicon cantilevers (NanoAndMore GmbH, k = 40 N m^{-1}, f = 300 kHz) with silicon tips (tip radius < 10 nm).

2.3. Synthetic Procedures

Carboxylic acid terminated poly(ethylene-*co*-butylene) **P1.** Hydroxyl terminated telechelic poly(ethylene-*co*-butylene) (5.00 g, 1.6 mmol), succinic anhydride (1.61 g, 16.0 mmol, 5.0 eq./end-group), and 4-dimethylaminopyridine (0.39 g, 3.2 mmol, 1.0 eq./end-group) were placed in a 100 mL round-bottomed flask equipped with a magnetic stirrer under nitrogen atmosphere. Anhydrous chloroform (50 mL) was added and the mixture was stirred at room temperature until all reagents completely dissolved. Anhydrous pyridine (1.30 mL, 16.0 mmol, 5.0 eq./end-group) was subsequently added via a syringe and the reaction mixture was stirred for 20 h at room temperature. Chloroform was then partially removed (≈40 mL) under reduced pressure and the concentrated chloroform solution was precipitated twice in 300 mL of methanol at room temperature. The product was dissolved in 200 mL of hexane, washed sequentially with 100 mL of HCl (5%) and brine, and dried over Na_2SO_4. Removal of the solvent under reduced pressure afforded carboxylic acid terminated poly(ethylene-*co*-butylene) **P1** as a colorless oil (3.2 g, 60%). ^{1}H-NMR ($CDCl_3$, 360 MHz,): δ (ppm) = 0.83 (t, J = 6.7 Hz, CH_3 backbone), 0.95–2.25 (m, CH_2 and CH backbone), 2.57–2.74 (m, CO−CH_2−CH_2−CO), 4.05–4.18 (m, COO−CH_2−). The ^{1}H-NMR spectrum shows residual alkene signals between 5.3 and 4.6 ppm. This is due to the fact that Krasol HLBH-P is industrially produced via hydrogenation of hydroxyl terminated polybutadiene, and the hydrogenation extent is slightly batch-dependent. M_n = 6.5 kDa; the molecular weight is higher than expected as a result of fractionation during the precipitation steps.

P2. P1 (80 mg, 23 µmol, 1.0 eq.), isobutyraldehyde **1b** (8.4 µL, 6.6 mg, 92 µmol, 4.0 eq.) and *tert*-butyl isocyanide **2a** (10 µL, 7.7 mg, 92 µmol, 4.0 eq.) were dissolved in 0.5 mL dichloromethane (DCM) and the reaction mixture was stirred for 24 h at room temperature. Direct precipitation in 40 mL methanol yielded the pure product as a colorless oil (80 mg, 91%). ^{1}H-NMR ($CDCl_3$, 300 MHz): δ (ppm) = 0.83 (t, J = 6.5 Hz, CH_3

backbone), 0.92 (d, J = 6.8 Hz, 6 H, 2 CHCH_3), 0.93 (d, J = 6.9 Hz, 6 H, 2 CHCH_3), 0.97–2.25 (m, CH_2 and CH backbone), 1.37 (s, 18 H, 2 ^{t}Bu), 2.28–2.42 (m, 2 H, 2 CH(CH_3)$_2$), 2.58–2.78 (m, 8 H, 4 CH_2CO), 4.03–4.16 (m, 4 H, 2 COOCH_2), 4.98 (d, J = 3.3 Hz, 2 H, 2 OCH), 6.13 (bs, 2 H, 2 NH).

P3. P1 (80 mg, 23 µmol, 1.0 eq.), acetaldehyde **1a** (5.0 µL, 4.1 mg, 92 µmol, 4.0 eq.) and *tert*-butyl isocyanide **2a** (10 µL, 7.7 mg, 92 µmol, 4.0 eq.) were dissolved in 0.5 mL DCM and the reaction mixture was stirred for 24 h at room temperature. Direct precipitation in 40 mL methanol yielded the pure product as colorless oil (74 mg, 86%). ^{1}H-NMR ($CDCl_3$, 300 MHz): δ (ppm) = 0.83 (t, J = 6.7 Hz, CH_3 backbone), 0.92–2.30 (m, CH_2 and CH backbone), 1.37 (s, 18 H, 2 ^{t}Bu), 1.44 (d, J = 6.8 Hz, 6 H, 2 CH_3), 2.52–2.80 (m, 8 H, 4 CH_2CO), 4.02–4.19 (m, 4 H, 2 COOCH_2), 5.13 (q, J = 6.8 Hz, 2 H, 2 OCH), 6.16 (bs, 2 H, 2 NH).

P4. P1 (80 mg, 23 µmol, 1.0 eq.), acetaldehyde **1a** (5.0 µL, 4.1 mg, 92 µmol, 4.0 eq.), and benzyl isocyanide **2b** (11 µL, 11 mg, 92 µmol, 4.0 eq.) were dissolved in 0.5 mL DCM and the reaction mixture was stirred for 24 h at room temperature. Direct precipitation in 40 mL methanol yielded the pure product as brown oil (67 mg, 76%). ^{1}H-NMR ($CDCl_3$, 300 MHz): δ (ppm) = 0.82 (t, J = 6.6 Hz, CH_3 backbone), 0.92–2.29 (m, CH_2 and CH backbone), 1.52 (d, J = 6.9 Hz, 6 H, 2 CH_3), 2.50–2.79 (m, 8 H, 4 CH_2CO), 3.81–4.02 (m, 4 H, 2 COOCH_2), 4.37–4.56 (m, 4 H, 2 NCH_2Ar), 5.32 (q, J = 6.8 Hz, 2 H, 2 OCH), 6.99 (bs, 2 H, 2 NH), 7.21–7.42 (m, 10 H, 10 Ar-H).

P5. P1 (400 mg, 114 µmol, 1.0 eq.), phenylacetaldehyde **1c** (53.5 µL, 54.9 mg, 457 µmol, 4.0 eq.) and benzyl isocyanide **2b** (55.7 µL, 53.5 mg, 457 µmol, 4.0 eq.) were dissolved in 2.5 mL DCM and the reaction mixture was stirred for 24 h at room temperature. Direct precipitation in 200 mL methanol yielded the pure product as yellow oil (361 mg, 79%). ^{1}H-NMR ($CDCl_3$, 300 MHz): δ (ppm) = 0.83 (t, J = 6.6 Hz, CH_3 backbone), 0.95–2.26 (m, CH_2 and CH backbone), 2.44–2.73 (m, 8 H, 4 CH_2CO), 3.17 (dd, J = 14.4, 7.3 Hz, 2 H, 2 CHCH^a_2Ar), 3.31 (dd, J = 14.3, 4.2 Hz, 2 H, 2 CHCH^b_2Ar), 3.78–3.96 (m, 4 H, 2 COOCH_2), 4.31 (dd, J = 15.0, 5.0 Hz, 2 H, 2 NCH^a_2Ar), 4.51 (dd, J = 14.8, 6.3 Hz, 2 H, 2 NCH^b_2Ar), 5.45–5.54 (m, 2 H, 2 OCH), 6.82–6.93 (bs, 2 H, 2 NH), 7.08–7.35 (m, 20 H, 20 Ar-H).

P6. P1 (80 mg, 23 µmol, 1.0 eq.), acetaldehyde **1a** (5.0 µL, 4.1 mg, 92 µmol, 4.0 eq.), and 2-naphthyl isocyanide **2c** (14 mg, 92 µmol, 4.0 eq.) were dissolved in 0.5 mL DCM and the reaction mixture was stirred for 24 h at room temperature. Direct precipitation in 40 mL methanol yielded the pure product as colorless oil (64 mg, 71%). ^{1}H-NMR ($CDCl_3$, 300 MHz): δ (ppm) = 0.82 (t, J = 6.6 Hz, CH_3 backbone), 0.93–2.28 (m, CH_2 and CH backbone), 1.62 (d, J = 6.9 Hz, 6 H, 2 CH_3), 2.56–2.93 (m, 8 H, 4 CH_2CO), 4.01–4.24 (m, 4 H, 2 COOCH_2), 5.47 (q, J = 6.8 Hz, 2 H, 2 OCH), 7.34–7.49 (m, 4 H, 4 H_d), 7.65–7.73 (m, 2 H, 2 H_c), 7.73–7.82 (m, 6 H, 6 H_b), 8.38 (s, 2 H, 2 H_a), 8.61 (bs, 2 H, 2 NH).

P7. P1 (322 mg, 92 µmol, 1.0 eq.), lauric aldehyde **1d** (82 µL, 68 mg, 368 µmol, 4.0 eq.) and octadecyl isocyanide **2d** (103 mg, 368 µmol, 4.0 eq.) were dissolved in 2.0 mL DCM and the reaction mixture was stirred for 24 h at room temperature. Direct precipitation in 160 mL methanol yielded the pure product as colorless oil (273 mg, 67%); T_m = 13.2 °C. ^{1}H-NMR ($CDCl_3$, 300 MHz): δ (ppm) = 0.83 (t, J = 6.7 Hz, CH_3 backbone), 0.88 (t, J = 6.3 Hz, 12 H, 4 CH_3), 0.92–2.29 (m, CH_2 and CH backbone + 52 CH_2), 2.52–2.84 (m, 8 H, 4 CH_2CO), 3.12–3.36 (m, 4 H, 2 NCH_2), 4.02–4.18 (m, 4 H, 2 COOCH_2), 5.13–5.22 (m, 2 H, 2 OCH), 6.56 (bs, 2 H, 2 NH).

P8. P1 (320 mg, 91 µmol, 1.0 eq.), lauric aldehyde **1d** (81 µL, 68 mg, 366 µmol, 4.0 eq.), and 1-isocyanodocosane **2e** (123 mg, 366 µmol, 4.0 eq.) were dissolved in 2.0 mL DCM and the reaction mixture was stirred for 24 h at room temperature. Flash silica column chromatography of the crude product (hexane/ethyl acetate 30:1, then DCM) yielded the pure product as colorless oil (301 mg, 73%); T_m = 30.7 °C. ^{1}H-NMR ($CDCl_3$, 300 MHz): δ (ppm) = 0.82 (t, J = 6.7 Hz, CH_3 backbone), 0.88 (t, J = 6.3 Hz, 12 H, 4 CH_3), 0.92–2.29 (m, CH_2 and CH backbone + 60 CH_2), 2.52–2.81 (m, 8 H, 4 CH_2CO), 3.13–3.35 (m, 4 H, 2 NCH_2), 4.03–4.16 (m, 4 H, 2 COOCH_2), 5.15–5.22 (m, 2 H, 2 OCH), 6.56 (bs, 2 H, 2 NH).

P9. P1 (320 mg, 91 µmol, 1.0 eq.), acetaldehyde **1a** (21 µL, 16 mg, 366 µmol, 4.0 eq.), and 1-isocyanodocosane **2e** (123 mg, 366 µmol, 4.0 eq.) were dissolved in 2.0 mL DCM and the reaction mixture was stirred for 24 h at room temperature. Flash silica column chromatography of the crude product (hexane/ethyl acetate 10:1, then DCM) yielded the pure product as colorless oil (279 mg, 72%); T_m = 39.3 °C. ^{1}H-NMR ($CDCl_3$, 300 MHz): δ (ppm) = 0.82 (t, J = 6.7 Hz, CH_3 backbone), 0.88 (t, J = 6.3 Hz, 6 H, 2 CH_3), 0.92–2.29 (m, CH_2 and CH backbone + 40 CH_2), 1.48 (d, J = 6.9 Hz, 6 H, 2 CH_3), 2.52–2.83 (m, 8 H, 4 CH_2CO), 3.16–3.33 (m, 4 H, 2 NCH_2), 4.03–4.19 (m, 4 H, 2 COOCH_2), 5.25 (q, J = 6.9 Hz, 2 H, 2 OCH), 6.57 (bs, 2 H, 2 NH).

P10. A solution of propylamine **3a** (7.6 µL, 5.5 mg, 92 µmol, 4.0 eq.) and isobutyraldehyde **1b** (8.4 µL, 6.6 mg, 92 µmol, 4.0 eq.) in 0.5 mL methanol was stirred for 1 h at room temperature. Then, **P1** (80 mg, 23 µmol, 1.0 eq.) in 0.5 mL THF and *tert*-butyl isocyanide **2a** (10.4 µL, 7.7 mg, 92 µmol, 4.0 eq.) were added. The mixture was stirred for 24 h. After removing the solvent in vacuo, the crude product was dissolved in 0.5 mL DCM and precipitated in 40 mL methanol. The pure product was obtained as colorless oil (80 mg, 88%). ^{1}H-NMR ($CDCl_3$, 300 MHz): δ (ppm) = 0.83 (t, J = 6.5 Hz, CH_3 backbone + 2 CH_2CH_3), 0.95 (d, J = 6.4 Hz, 12 H, 2 CH(CH_3)$_2$), 0.91–2.23 (m, CH_2 and CH backbone + 2 CH_2CH$_3$), 1.30 (s, 18 H, 2 ^{t}Bu), 2.32–2.50 (m, 2 H, 2 CH(CH_3)$_2$), 2.56–2.78 (m, 8 H, 4 CH_2CO), 3.26 (t, J = 8.2 Hz, 4 H, 2 NCH_2), 3.93–4.18 (m, 6 H, 2 NCH, 2 COOCH_2), 6.48 (bs, 2 H, 2 NH).

P11. A solution of propylamine **3a** (7.6 µL, 5.5 mg, 92 µmol, 4.0 eq.) and isobutyraldehyde **1b** (8.4 µL, 6.6 mg, 92 µmol, 4.0 eq.) in 0.5 mL methanol was stirred for 1 h at room temperature. Then, **P1** (80 mg, 23 µmol, 1.0 eq.) in 0.5 mL THF and benzyl isocyanide **2b** (11 µL, 11 mg, 92 µmol, 4.0 eq.) were added. The mixture was stirred for 24 h. After removing the solvent in vacuo, the crude product was dissolved in 0.5 mL DCM and precipitated in 40 mL methanol. The pure product was obtained as colorless oil (78 mg, 86%). ^{1}H-NMR ($CDCl_3$, 300 MHz): δ (ppm) = 0.82 (t, J = 6.6 Hz, CH_3 backbone + 2 CH_2CH_3), 0.98 (d, J = 6.4 Hz, 12 H, 2 CH(CH_3)$_2$), 1.00–2.27 (m, CH_2 and CH backbone + 2 CH_2CH$_3$), 2.42–2.62 (m, 2 H, 2 CH(CH_3)$_2$), 2.56–2.77 (m, 8 H, 4 CH_2CO), 3.15–3.36 (m, 4 H, 2 NCH_2CH$_3$), 3.98–4.25 (m, 6 H, 2 NCH, 2 COOCH_2), 4.30–4.49 (m, 4 H, 2 NCH_2Ar), 7.12 (bs, 2 H, 2 NH), 7.17–7.35 (m, 10 H, 10 Ar-H).

P12. A solution of octadecylamine **3b** (99.0 mg, 368 µmol, 4.00 eq.) and isobutyraldehyde **1b** (34.0 µL, 26.5 mg, 368 µmol, 4.00 eq.) in 2.0 mL methanol was stirred for 1 h at room temperature. Then, **P1** (322 mg, 92.0 µmol, 1.00 eq.) in 2.0 mL THF and octadecyl isocyanide **2d** (103 mg, 368 µmol, 4.00 eq.) were added. The mixture was stirred for 24 h. After removing the solvent in vacuo, the crude product was dissolved in 1.5 mL DCM and precipitated in 160 mL methanol. The pure product was obtained as yellowish oil (222 mg, 51.3%); T_m = 16.4 °C. ^{1}H-NMR ($CDCl_3$, 300 MHz): δ (ppm) = 0.82 (t, J = 6.8 Hz, CH_3 backbone), 0.88 (t, J = 6.3 Hz, 12 H, 4 CH_3), 0.95 (d, J = 6.4 Hz, 12 H, 2 $CH(CH_3)_2$), 0.94–2.28 (m, CH_2 and CH backbone + 64 CH_2), 2.37–2.56 (m, 2 H, 2 $CH(CH_3)_2$), 2.56–2.75 (m, 8 H, 4 CH_2CO), 3.16 (dd, J = 13.2, 6.7 Hz, 4 H, 2 $CONCH_2$), 3.21–3.40 (m, 4 H, 2 $CONHCH_2$), 3.93–4.19 (m, 6 H, 2 NCH, 2 $COOCH_2$), 6.69 (bs, 2 H, 2 NH).

3. Results and Discussion

Telechelic poly(ethylene-*co*-butylene)s (PEBs) containing amide end-groups were synthesized from carboxylic acid terminated telechelic PEB **P1** (M_n = 6.5 kDa; $Đ$ = 1.13, **Scheme 1**), which was obtained by base-catalyzed ring opening of succinic anhydride with hydroxyl terminated telechelic PEB. The Passerini or Ugi reaction of **P1** was performed with well-established components used in previous studies[41,43,44] including aldehydes **1a–1c**, isocyanides **2a–2c**, and amine **3a** (Scheme 1). In addition, we introduced less common components exhibiting long aliphatic moieties (C_{12}–C_{22}) such as lauric aldehyde **1d**, isocyanides **2e** and **2f**, and octadecylamine **3b**. We also tested anthracene- and pyrenecarboxaldehyde; however, very low conversion of the acid end-groups was achieved using these aromatic aldehydes arguably due to their low solubility and inherent steric demand. The Passerini reactions were performed in dichloromethane and the Ugi reactions in a mixture of THF and methanol. Full conversion of the end-groups (within the limit of detection of ^{1}H-NMR) was achieved after 24 h by performing the reaction in highly concentrated solution and using an excess of the components (two equivalents per acid end-group). Thus, amide-functionalized telechelics **P2–P12** were obtained in good yields and considered for further characterization (Scheme 1 and **Table 1**).

The successful synthesis of **P2–P12** was proven by ^{1}H-NMR; **Figure 1** shows the assigned spectra of **P1** (for reference) as well as **P7**, **P9**, and **P12** as representative examples. The spectra of all other products can be found in the Supporting Information. The synthesized telechelics display the characteristic signal of the amide NH proton at ≈6.6 ppm and all the other expected signals for each newly formed end-group, which could be unambiguously assigned. Besides, the signals of the new end-groups display the expected integrals ratio (see the Supporting Information) with respect to the α-hydrogens of the ester functional group of **P1** (protons *a* in Figure 1), which indicates that the carboxylic acid end-groups are fully converted (within the detection limit of ^{1}H-NMR). The corresponding SEC-traces of **P2–P12** indicate a shift to higher molecular weights while keeping a narrow molecular weight distribution (**Figure 2** and the Supporting Information).

The microstructure of telechelic PEBs **P2–P12** was first investigated via DSC. All polymers show the glass transition temperature of the PEB backbone at ≈–50 °C (Table 1); however, only four of them (**P7**, **P8**, **P9**, and **P12**) display an additional melting endotherm characteristic of a phase segregated structure (Table 1 and **Figure 3**). The melting temperatures of these polymers range from 13 to 39 °C and **P8** and **P9** form self-standing films at room temperature. We further analyzed these four polymers via SAXS at –20 °C, i.e., well below their melting temperatures, and in all cases observed correlation peaks indicative of a microphase segregated morphology with short range order (**Figure 4**). The calculated domain spacings are 9.7 nm for **P7**, 8.7 nm for **P8**, 11.6 nm for **P9**, and 11.2 nm for **P12**.

Unlike **P7**, **P8**, **P9**, and **P12**, which phase segregate as a result of end-group crystallization, all other telechelic PEBs were found to be fully amorphous regardless of any attempts

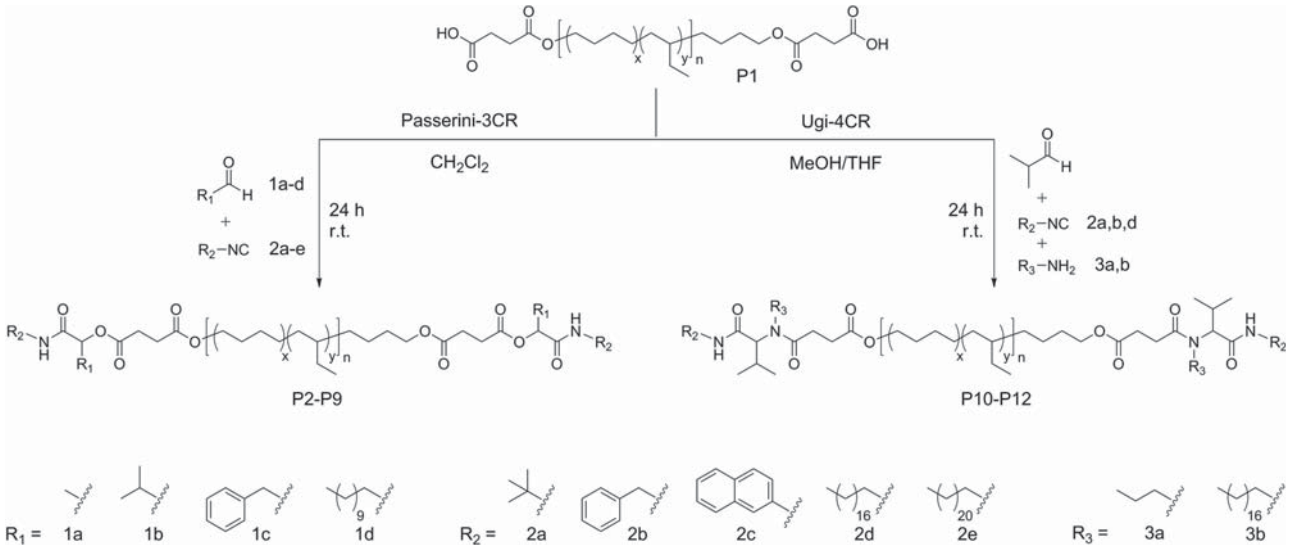

Scheme 1. Synthesis of amide terminated telechelic poly(ethylene-*co*-butylene)s **P2–P12** via Passerini and Ugi multicomponent reactions.

Table 1. SEC and thermal data of telechelic PEBs P1-P12.

Polymer	End-group	M_n [kDa]/$Đ$	T_g/T_m [°C]	Polymer	End-group	M_n [kDa]/$Đ$	T_g/T_m [°C]
P1		6.5/1.13	–55/–	**P7**	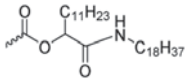	8.4/1.04	–55/13
P2	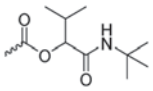	7.2/1.08	–57/–	**P8**	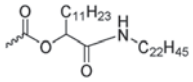	8.7/1.08	–52/31
P3	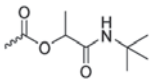	7.2/1.08	–55/–	**P9**	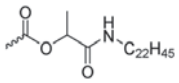	8.3/1.07	–51/39
P4	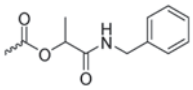	7.1/1.09	–54/–	**P10**	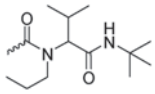	6.7/1.18	–53/–
P5	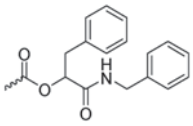	7.2/1.09	–50/–	**P11**	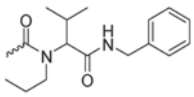	7.0/1.13	–56/–
P6	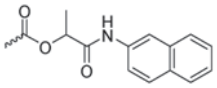	7.1/1.09	–49/–	**P12**	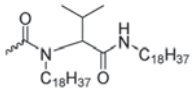	8.7/1.05	–52/16

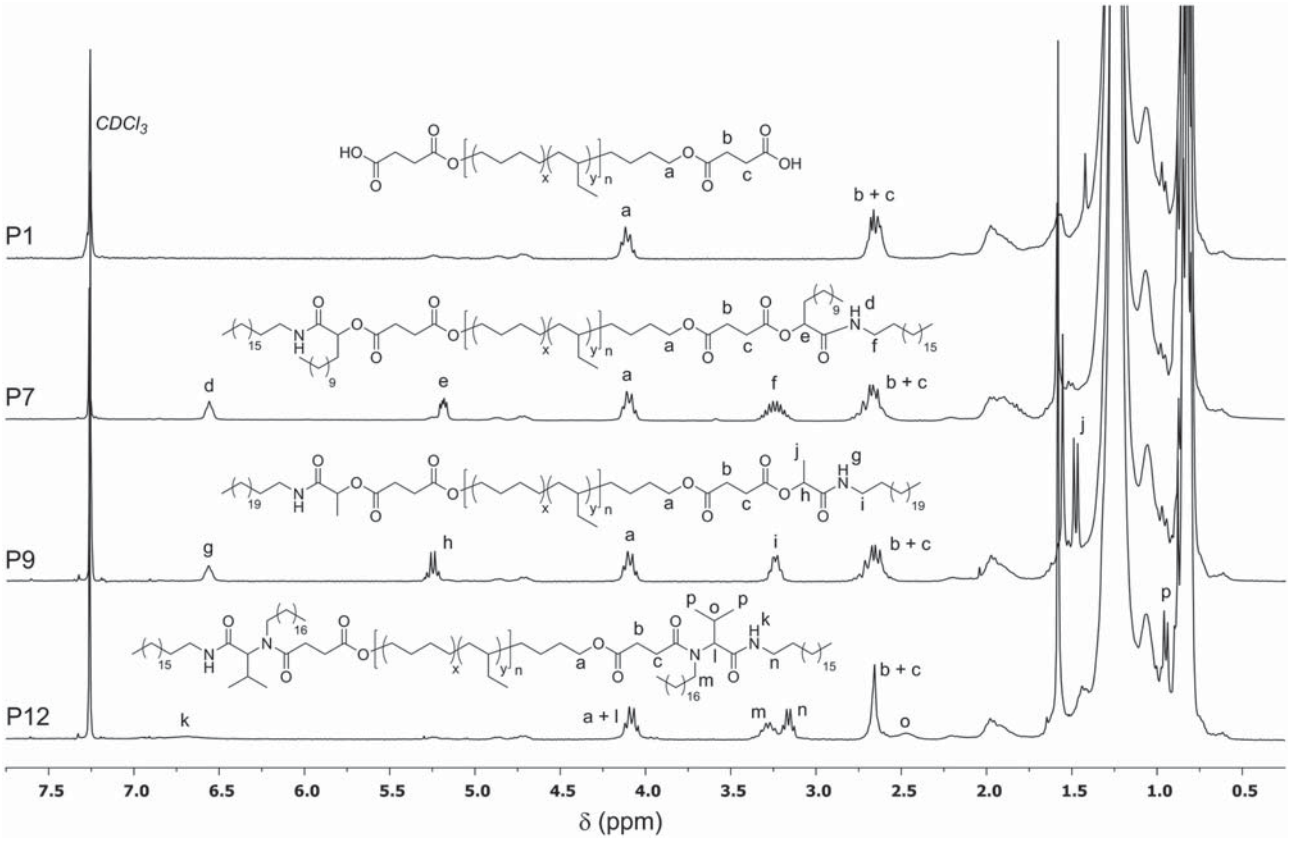

Figure 1. ^{1}H-NMR spectra of carboxylic acid terminated PEB **P1** and amide terminated telechelic PEBs **P7**, **P9,** and **P12** (the spectra of all other telechelics are shown in the Supporting Information). The low intensity signals between 4.6 and 5.3 ppm are residual alkene groups already present in the commercial hydroxyl terminated PEB.

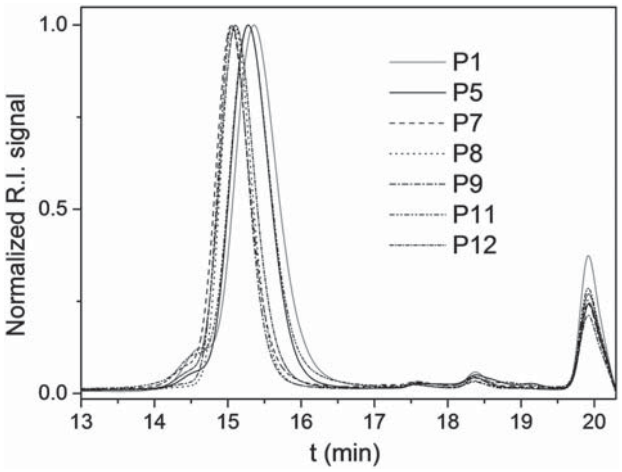

Figure 2. SEC traces of carboxylic acid terminated PEB **P1** and selected telechelic PEBs synthesized via Passerini and Ugi MCRs.

to anneal them. **P7**, **P8**, **P9**, and **P12** have in common the presence of long aliphatic chains, which appear to promote crystallization much more efficiently than other groups such as benzyl (**P4**, **P5**, and **P11**) or naphthyl (**P6**). These observations are in sharp contrast to the crystallinity of previously reported small molecules with similar functionalities synthesized via Passerini and Ugi MRCs,[43,44] and suggest a strong influence of the molar fraction of the end-groups on their aggregation and crystallization. Indeed, the end-group molar fraction in **P7**, **P8**, **P9**, and **P12** varies between 12 and 17 mol%, while that of the polymers that did not show microphase segregation oscillates between 7 and 10 mol%. The reduced concentration of motifs in the associated state appears to prevent their crystallization into a separate hard phase.

The nanostructure of **P9** was subsequently investigated by AFM. **Figure 5** shows the height and phase images recorded on the surface of a sample that was melt-cast, cooled to –20 °C for 12 h (same procedure as for the SAXS analysis) and stored inside a desiccator at ambient temperature. The micrograph reveals a nonordered fibril-like nanostructure in agreement with the presence of two phases which, according to the phase image, display clearly different stiffness. These observations are in line with the DSC and SAXS data, and support our conclusion that these telechelics phase segregate into a soft PEB phase and a stiff crystalline phase. In addition, the spacing between adjacent fibrils (see the Supporting Information for profiles) is in good agreement with the domain spacing obtained by SAXS (11.6 nm).

Besides the end-group molar fraction, the absence of crystallization in some of these polymers shows that phase segregation in systems based on weakly H-bonding motifs, such as the amides studied here, requires of highly crystalline motifs or auxiliary functional groups that promote aggregation. Thus, the long alkyl chains in **P7**, **P8**, **P9,** and **P12** appear to induce phase segregation more efficiently than the other studied substituents. However, this observation triggers the question whether phase segregation takes place solely on the basis of alkyl chain crystallization or if this process is supported by amide–amide H-bonding. This was investigated by exposing **P9** (T_m = 39 °C) to trifluoroacetic acid (TFA) vapors at room temperature with the aim of selectively disrupting amide–amide H-bonds of the otherwise acid-inert structure. Such treatment transformed the initially solid sample into a viscous liquid in only 10 min (**Figure 6**), and the thermogram (first heating scan) of the product showed a decrease of the melting endotherm from 39 to 5 °C (Figure 6). On the second heating scan, the melting endotherm of **P9** was recovered as a result of TFA evaporation (Figure 6). These results suggest that long alkyl chains alone can promote phase segregation on the basis of their crystallinity and high molar fraction, and that hydrogen bonding does play an important role on the crystallization behavior of these amide-functionalized PEB-based telechelics. Indeed, hydrogen bonding groups such as urea and urethane have already been shown to induce the crystallization of supramolecular motifs attached to the termini of very similar telechelics[45] and, in the present case, the amide groups seem to play the same role by templating the crystallization of the alkyl chains, which results in an increase of the melting temperature.

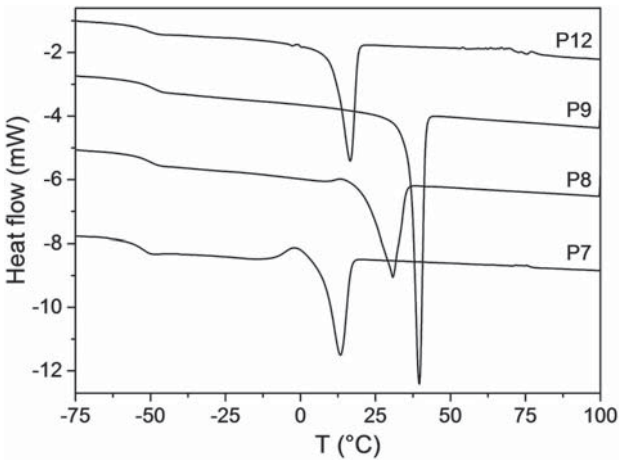

Figure 3. Thermograms (first heating scans) of telechelic PEBs **P7**, **P8**, **P9,** and **P12**.

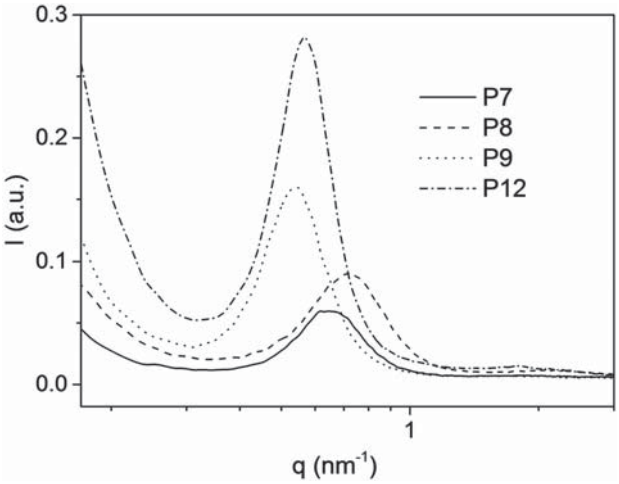

Figure 4. SAXS spectra of telechelic PEBs **P7**, **P8**, **P9,** and **P12** equilibrated at –20 °C for 12 h.

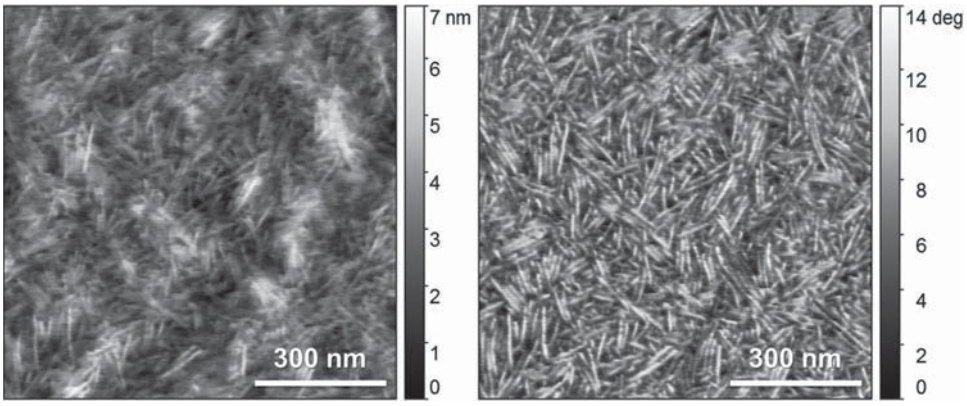

Figure 5. AFM height (left) and phase (right) images of **P9**.

Overall, this work widens the application scope of the Passerini and Ugi MCRs with the synthesis of functional telechelics. Especially useful is the possibility of rapidly screening very diverse amide end-groups that these MCRs offer, which provides a new insight into the structure-property relationships of this kind of materials.

4. Conclusions

In this work, we have used the Passerini and Ugi multicomponent reactions to obtain a library of telechelic poly(ethylene-*co*-butylene)s bearing amide functionalities at both termini. This synthetic approach allowed varying the composition and size of the end-groups, and studying the effect of these parameters on the phase segregation behavior of the resulting telechelics. The introduction of small amide derivatives containing alkyl, benzyl, or naphthyl groups resulted in nonphase segregated telechelics. On the other hand, the end-group functionalization with amide groups displaying long alkyl chains provided phase segregated materials, which suggests that the end-group's molar fraction and the presence of crystalline residues play an important role on the segregation of the polar, hydrogen bonding amide end-groups from the soft poly(ethylene-*co*-butylene) core. Two of these materials display hard phase melting temperatures over 30 °C and thus form self-standing films at room temperature. Apart from being highly thermosensitive, these materials lose their mechanical integrity when exposed to a H-bonding competitor such as TFA (vapor), but recover their properties once it evaporates.

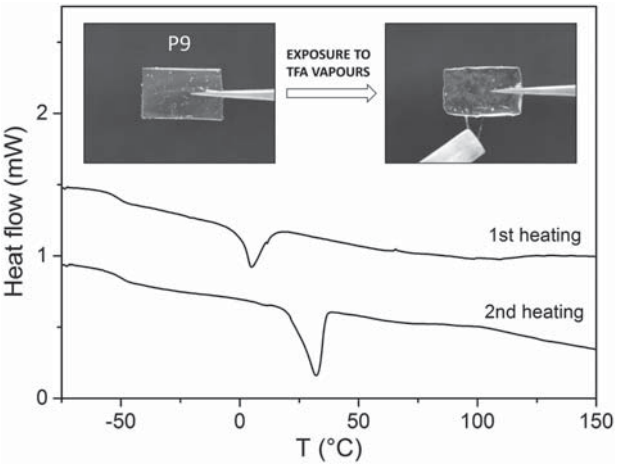

Figure 6. The pictures show a film of **P9** before and after exposure to TFA vapors at room temperature for 10 min. The first and second heating scans (DSC traces) of **P9** after exposure to TFA vapors are also shown.

Supporting Information

Supporting Information is available from the Wiley Online Library or from the author.

Acknowledgements

The authors acknowledge financial support from the Adolphe Merkle Foundation. L.M.E. is grateful for support through the Ambizione program of the Swiss National Science Foundation (SNSF). This project also received funding from the European Union's Horizon 2020 research and innovation programme under the Marie Sklodowska-Curie Grant Agreement No 706329/cOMPoSe (I.G.) Sandor Balog (Adolphe Merkle Institute) is acknowledged for SAXS analyses. The authors are thankful to Felix Mack for experimental support.

Conflict of Interest

The authors declare no conflict of interest.

Keywords

Passerini reaction, phase-segregated polymers, stimuli-responsive polymers, supramolecular polymers, Ugi reaction

[1] L. Yang, X. Tan, Z. Wang, X. Zhang, *Chem. Rev.* **2015**, *115*, 7196.
[2] X. Yan, F. Wang, B. Zheng, F. Huang, *Chem. Soc. Rev.* **2012**, *41*, 6042.

[3] R. J. Wojtecki, M. A. Meador, S. J. Rowan, *Nat. Mater.* **2011**, *10*, 14.
[4] L. Montero de Espinosa, G. L. Fiore, C. Weder, E. Johan Foster, Y. C. Simon, *Prog. Polym. Sci.* **2015**, *49–50*, 60.
[5] C. Heinzmann, C. Weder, L. M. de Espinosa, *Chem. Soc. Rev.* **2015**.
[6] R. P. Sijbesma, F. H. Beijer, L. Brunsveld, B. J. B. Folmer, J. H. K. K. Hirschberg, R. F. M. Lange, J. K. L. Lowe, E. W. Meijer, *Science* **1997**, *278*, 1601.
[7] B. J. B. Folmer, R. P. Sijbesma, R. M. Versteegen, J. A. J. van der Rijt, E. W. Meijer, *Adv. Mater.* **2000**, *12*, 874.
[8] J. H. K. K. Hirschberg, F. H. Beijer, H. A. van Aert, P. C. M. M. Magusin, R. P. Sijbesma, E. W. Meijer, *Macromolecules* **1999**, *32*, 2696.
[9] U. S. Schubert, C. Eschbaumer, *Angew. Chem., Int. Ed.* **2002**, *41*, 2892.
[10] M. Burnworth, L. Tang, J. R. Kumpfer, A. J. Duncan, F. L. Beyer, G. L. Fiore, S. J. Rowan, C. Weder, *Nature* **2011**, *472*, 334.
[11] D. W. R. Balkenende, C. A. Monnier, G. L. Fiore, C. Weder, *Nat. Commun.* **2016**, *7*, 10995.
[12] L. Brunsveld, B. J. B. Folmer, E. W. Meijer, R. P. Sijbesma, *Chem. Rev.* **2001**, *101*, 4071.
[13] R. J. Wojtecki, A. Nelson, *J. Polym. Sci., Part A: Polym. Chem.* **2016**, *54*, 457.
[14] M. Müller, A. Dardin, U. Seidel, V. Balsamo, B. Iván, H. W. Spiess, R. Stadler, *Macromolecules* **1996**, *29*, 2577.
[15] L. de Lucca Freitas, M. M. Jacobi, G. Gonçalves, R. Stadler, *Macromolecules* **1998**, *31*, 3379.
[16] M. Schirle, I. Hoffmann, T. Pieper, H.-G. Kilian, R. Stadler, *Polym. Bull.* **1996**, *36*, 95.
[17] C. P. Lillya, R. J. Baker, S. Hutte, H. H. Winter, Y. G. Lin, J. Shi, L. C. Dickinson, J. C. W. Chien, *Macromolecules* **1992**, *25*, 2076.
[18] D. Duweltz, F. Lauprêtre, S. Abed, L. Bouteiller, S. Boileau, *Polymer* **2003**, *44*, 2295.
[19] S. Sivakova, D. A. Bohnsack, M. E. Mackay, P. Suwanmala, S. J. Rowan, *J. Am. Chem. Soc.* **2005**, *127*, 18202.
[20] J. Cortese, C. Soulié-Ziakovic, M. Cloitre, S. Tencé-Girault, L. Leibler, *J. Am. Chem. Soc.* **2011**, *133*, 19672.
[21] S. J. Rowan, P. Suwanmala, S. Sivakova, *J. Polym. Sci., Part A: Polym. Chem.* **2003**, *41*, 3589.
[22] D. H. Merino, A. Feula, K. Melia, A. T. Slark, I. Giannakopoulos, C. R. Siviour, C. P. Buckley, B. W. Greenland, D. Liu, Y. Gan, P. J. Harris, A. M. Chippindale, I. W. Hamley, W. Hayes, *Polymer* **2016**, *107*, 368.
[23] P. Woodward, D. H. Merino, I. W. Hamley, A. T. Slark, W. Hayes, *Aust. J. Chem.* **2009**, *62*, 790.
[24] L. Montero de Espinosa, S. Balog, C. Weder, *ACS Macro Lett.* **2014**, *3*, 540.
[25] C. L. Elkins, K. Viswanathan, T. E. Long, *Macromolecules* **2006**, *39*, 3132.
[26] B. D. Mather, M. B. Baker, F. L. Beyer, M. A. G. Berg, M. D. Green, T. E. Long, *Macromolecules* **2007**, *40*, 6834.
[27] P. J. Woodward, D. Hermida Merino, B. W. Greenland, I. W. Hamley, Z. Light, A. T. Slark, W. Hayes, *Macromolecules* **2010**, *43*, 2512.
[28] D. H. Merino, A. T. Slark, H. M. Colquhoun, W. Hayes, I. W. Hamley, *Polym. Chem.* **2010**, *1*, 1263.
[29] I. Ugi, C. Steinbrückner, *Angew. Chem.* **1960**, *72*, 267.
[30] M. Passerini, *Gazz. Chem. Ital.* **1921**, *51*, 126.
[31] *Multi-Component and Sequential Reactions in Polymer Synthesis*, Vol. *269* (Ed: P. Theato), Springer International Publishing, Switzerland **2015**.
[32] R. Kakuchi, *Angew. Chem., Int. Ed.* **2014**, *53*, 46.
[33] S. Wang, C. Fu, Y. Wei, L. Tao, *Macromol. Chem. Phys* **2014**, *215*, 486.
[34] R. Hu, W. Li, B. Z. Tang, *Macromol. Chem. Phys* **2016**, *217*, 213.
[35] M. Hartweg, C. R. Becer, *Green Chem.* **2016**, *18*, 3272.
[36] H. Xue, Y. Zhao, H. Wu, Z. Wang, B. Yang, Y. Wei, Z. Wang, L. Tao, *J. Am. Chem. Soc.* **2016**, *138*, 8690.
[37] J. G. Rudick, *J. Polym. Sci., Part A: Polym. Chem.* **2013**, *51*, 3985.
[38] O. Kreye, D. Kugele, L. Faust, M. A. R. Meier, *Macromol. Rapid. Commun.* **2014**, *35*, 317.
[39] S. C. Solleder, K. S. Wetzel, M. A. R. Meier, *Polym. Chem.* **2015**, *6*, 3201.
[40] S. C. Solleder, D. Zengel, K. S. Wetzel, M. A. R. Meier, *Angew. Chem., Int. Ed.* **2016**, *55*, 1204.
[41] A. Sehlinger, B. Verbraeken, M. A. R. Meier, R. Hoogenboom, *Polym. Chem.* **2015**, *6*, 3828.
[42] Y. Zhang, Y. Zhao, B. Yang, C. Zhu, Y. Wei, L. Tao, *Polym. Chem.* **2014**, *5*, 1857.
[43] A. Sehlinger, K. Ochsenreither, N. Bartnick, M. A. R. Meier, *Eur. Polym. J.* **2015**, *65*, 313.
[44] A. Sehlinger, O. Kreye, M. A. R. Meier, *Macromolecules* **2013**, *46*, 6031.
[45] H. Kautz, D. J. M. van Beek, R. P. Sijbesma, E. W. Meijer, *Macromolecules* **2006**, *39*, 4265.